Title

Photocatalytic Color Switching of Transition Metal Hexacyanometalate Nanoparticles for High-Performance Light-Printable Rewritable Paper

Journal

Nano Letters, 17(2)

ISSN

1530-6984

Authors

Wang, Wenshou
Feng, Ji
Ye, Yifan
et al.

Publication Date

2017-02-08

DOI

10.1021/acs.nanolett.6b03909

Peer reviewed

NANO LETTERS

Letter

pubs.acs.org/NanoLett

Photocatalytic Color Switching of Transition Metal Hexacyanometalate Nanoparticles for High-Performance Light-Printable Rewritable Paper

Wenshou Wang,*[,†,‡] Ji Feng,[‡] Yifan Ye,[§] Fenglei Lyu,[‡] Yi-sheng Liu,[§] Jinghua Guo,[§] and Yadong Yin*[,‡]

[†]National Engineering Research Center for Colloidal Materials and School of Chemistry and Chemical Engineering, Shandong University, Ji'Nan 250100, P. R. China

[‡]Department of Chemistry and UCR Center for Catalysis, University of California, Riverside, California 92521, United States

[§]Advanced Light Source, Lawrence Berkeley National Laboratory, Berkeley, California 94720, United States

S *Supporting Information*

ABSTRACT: Developing efficient photoreversible color switching systems for constructing rewritable paper is of significant practical interest owing to the potential environmental benefits including forest conservation, pollution reduction, and resource sustainability. Here we report that the color change associated with the redox chemistry of nanoparticles of Prussian blue and its analogues could be integrated with the photocatalytic activity of TiO_2 nanoparticles to construct a class of new photoreversible color switching systems, which can be conveniently utilized for fabricating ink-free, light printable rewritable paper with various working colors. The current system also addresses the phase separation issue of the previous organic dye-based color switching system so that it can be conveniently applied to the surface of conventional paper to produce an ink-free light printable rewritable paper that has the same feel and appearance as the conventional paper. With its additional advantages such as excellent scalability and outstanding rewriting performance (reversibility >80 times, legible time >5 days, and resolution >5 μm), this novel system can serve as an eco-friendly alternative to regular paper in meeting the increasing global needs for environment protection and resource sustainability.

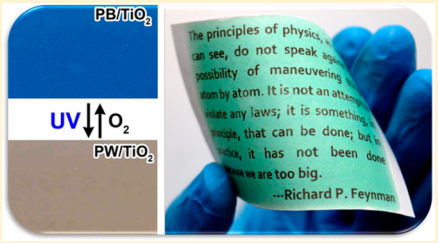

KEYWORDS: *Prussian blue, Prussian blue analogues, titania, nanoparticles, photoreversible color switching, rewritable paper*

Reversible light-responsive materials have attracted increasing attention because of their practical applications in color display, data storage, optoelectronic devices, sensors, and security systems.[1−8] Significant efforts have been previously made to the development of various chromophores capable of photoisomerization, which however still face challenges in practical uses due to limited reversibility and stability resulting from unavoidable thermal back relaxation, accumulation of side products, high cost due to complicated synthetic procedure, and toxicity.[9−16] Recently we have demonstrated a new photoreversible color switching system (PCSS) based on the color change of redox dyes in response to photocatalytic reactions of TiO_2 nanoparticles (NPs) under UV illumination.[17−19] Although several dyes such as methylene blue, acid green, and neutral red were found to be effective,[17] it has been challenging to achieve good color switching performance (in terms of, for example, resolution and repeatability) with other dyes because their redox chemistry is often not aligned with the photocatalytic property of TiO_2 NPs. In addition, the stability of redox dyes under repeated/prolonged UV irradiation remains a big issue which could eventually cause their partial degradation and subsequently limit the reversibility and color contrast of the system. Another significant challenge of the previous color switching system is that it can only be applied to nonporous substrates such as glass and plastic sheets. For porous substrates such as a conventional paper, the porous fibrous network will separate the dye molecules and the TiO_2 particles to prevent effective electron transfer and subsequently color switching. Therefore, it is highly desirable to develop a class of new redox-driven color switching materials with various accessible colors as the imaging media to cooperate with photocatalysts to enable a new color switching system for ink-free photoreversible printing, which is believed to have significant benefits in forest conservation, energy saving, and environmental protection.[20−28]

Prussian Blue (PB) and its analogues (PBAs), the well-known synthetic coordination compound of transition metal hexacyanometalates, typically possess a face-centered cubic crystal structure with the $Fm\bar{3}m$ space group, in which transition metal ions are linked together through cyanide ligands. PB and PBAs have been explored for a wide range of applications in pigments, electrochromic devices, sensors, catalysts, biomedicines, and batteries.[29−33] The transition metal hexacyanometalates display various colors in the visible region due to the charge transfer of the mixed valence state of transition metals and cyanide ligands. A well-known example

Received: September 18, 2016
Revised: November 21, 2016
Published: November 22, 2016

DOI: 10.1021/acs.nanolett.6b03909
Nano Lett. 2017, 17, 755−761

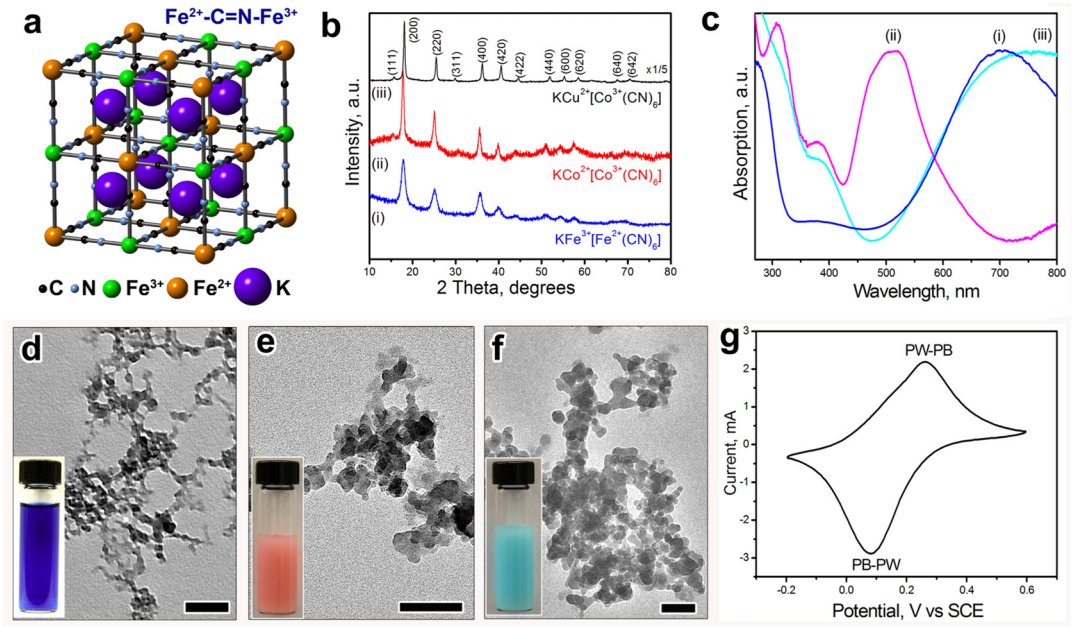

Figure 1. Structure and characterization of PB and PBA NPs. (a) Schematic illustration of a face-centered cubic structure of PB. Owing to the lengthy C≡N bonds, subunit cells contain large interstitial sites for cations such as K^+. (b) XRD patterns and (c) UV−vis absorption spectra of PB and PBA NPs: (i) PB, (ii) $KCo^{2+}[Co^{3+}(CN)_6]$, and (iii) $KCu^{2+}[Co^{3+}(CN)_6]$. (d−f) TEM images of PB (d), $KCo^{2+}[Co^{3+}(CN)_6]$ (e), and $KCu^{2+}[Co^{3+}(CN)_6]$ NPs (f). Scale bar: 100 nm. Inset in d−f: digital photographs of aqueous dispersions of PB, $KCo^{2+}[Co^{3+}(CN)_6]$, and $KCu^{2+}[Co^{3+}(CN)_6]$ NPs showing blue, red, and green colors, respectively. (g) Cyclic voltammogram of PB NPs in KCl solution at a scanning rate of 5 mV s^{-1}.

includes the "soluble" PB, which is in fact in colloidal form. It can be reduced from its deep blue color to the colorless form of Prussian white (PW) and then recovered by oxidation through the following reaction: $KFe^{3+}[Fe^{2+}(CN)_6] + K^+ + e^- \rightleftarrows K_2Fe^{2+}[Fe^{2+}(CN)_6]$.[34] Because of its excellent color switching properties between PB and PW under external electrical stimuli, PB has been considered as a prominent candidate for the electrochromic displays. Previous studies on these electrochromic devices have reported lifetimes in the range of 10^5 to over 10^7 cycles, suggesting extremely high stability for color switching.[35,36]

In this work, we take advantage of the great features of PB and PBAs and demonstrate their use in nanoparticular form as the imaging media to couple with photoreductive TiO_2 nanoparticles for constructing a new PCSS with various working colors. With the assistance of surface-bound sacrificial electron donors (SEDs), photoexcitation of the TiO_2 nanoparticles by UV illumination produces electrons on the particle surface and reduces the adjacent nanoparticles of PB or PBAs and subsequently change their color. The color may switch back completely through oxidation either slowly under ambient condition or rapidly upon mild heating. The current system can also effectively prevent phase separation of the two types of nanoparticles when cast onto the surfaces of a conventional paper, producing an ink-free light printable rewritable paper that has the same feel and appearance as the conventional paper, with additional advantages such as various working colors, excellent rewritability (>80 times), and consistently high color contrast. The printed patterns remain legible at ambient conditions for more than 5 days with high resolution, which is sufficiently long for most temporary reading purposes. In view of the excellent writing−erasing repeatability with high resolution and legibility, the applicability to conventional paper substrates, tailorable working colors, and low cost and low toxicity, we believe the new rewritable paper greatly surpasses the previous systems and holds great promises for practical applications to meet our society's increasing needs for achieving sustainability.

PB has a cubic framework with Fe^{2+} and Fe^{3+} cations on alternate corners of a cube of corner-shared octahedra bridged by linear $C{\equiv}N^-$ anions, with the low-spin Fe^{2+} bound to C atoms and the high-spin Fe^{3+} to N atoms (Figure 1a). The C≡N bond opens the faces of the elementary cubes for K^+ to move between half-filled body-center positions. The key to the successful realization of color switching of a redox compound by photocatalytic TiO_2 is to match its redox potential to that of the electrons photogenerated from TiO_2. Since the edge of the conduction band of TiO_2 (≈ −0.52 V vs SHE) is well above the redox potentials of both $Fe(CN)_6^{4-/3-}$ (≈0.36 V vs SHE) and $Fe^{3+/2+}$ (≈0.77 V vs SHE), the reduction of PB to PW is possible by the photogenerated electrons from TiO_2.[37,38] Interestingly, our recent work has shown that anatase TiO_2 NPs of several nanometers in size, capped with a polymeric ligand (Figure S1), poly(ethylene glycol)-*b*-poly(propylene glycol)-*b*-poly(ethylene glycol) (P123) as an effective SED, could become reductive upon UV light excitation and initiate the reduction reaction of redox dyes.[19] Since electron transfer plays a key role in the reduction reaction, it is very important to increase the contact between TiO_2 and PB NPs and ensure effective electron transfer, which can be achieved by synthesizing small and uniform PB NPs. Simply mixing aqueous solutions of $K_4[Fe(CN)_6]$ and metal salt such as $FeCl_3$, however, was only able to produce relatively large PB particles with a wide size distribution. We have addressed this issue by developing a new coprecipitation process using citric acid as small anion stabilizers, which can act as a capping agent to control the size and prevent agglomeration of PB NPs. This process results in relatively uniform PB NPs with an average

DOI: 10.1021/acs.nanolett.6b03909
Nano Lett. 2017, 17, 755−761

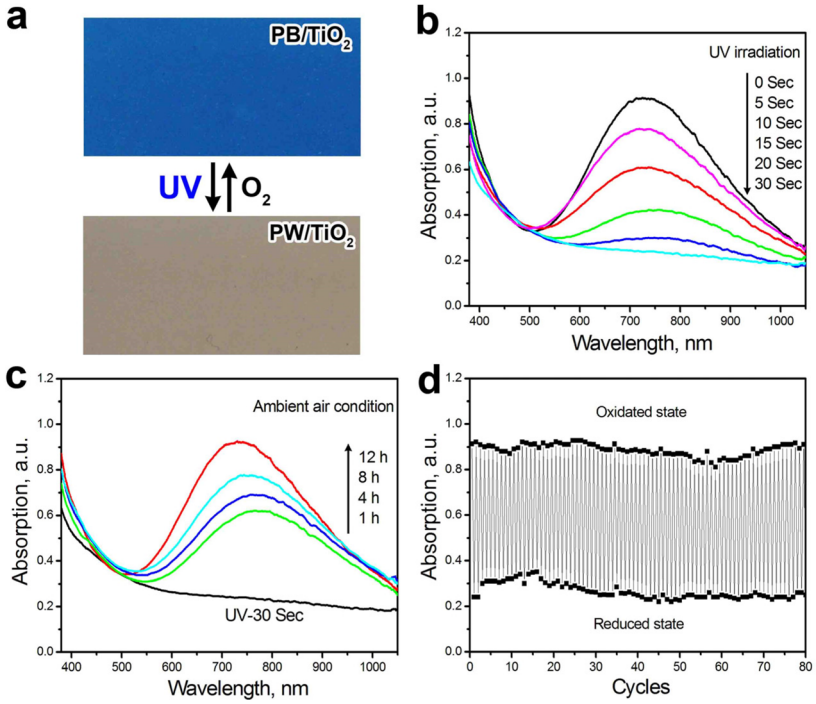

Figure 2. Photoreversible color switching and stability of the PB/TiO_2 solid film. (a) Digital images of a solid film showing the decoloration and recoloration process; (b) UV−vis spectra showing the decoloration process under UV irradiation; (c) UV−vis spectra showing the recoloration process at room temperature under ambient air; (d) the absorption intensity of a solid film recorded continuously in 80 cycles of switching between color and colorless states.

size of ∼16 nm, which exhibit brightly blue color with a strong absorption peak at ∼704 nm, as shown in the transmission electron microscopy (TEM) image and UV−vis absorption spectra (Figure 1c,d and Figure S2). The X-ray diffraction (XRD) pattern in Figure 1b shows that all diffraction peaks can be indexed to PB, which is consistent with the reported colloidal PB NPs.[39] The diffraction peaks are broadened due to the small size of PB NPs. Figure 1g gives a typical cyclic voltammogram of PB NPs with the applied voltage between −0.2 and 0.6 V relative to the reference electrode at a scanning rate of 5 mV s^{-1}. The CV curve shows a redox pair, in which the reduction peak is at 0.08 V and oxidation peak is at 0.26 V. This redox pair is associated with the electrochemical switching between PB and PW. The citric acid assisted coprecipitation method can be easily extended to the synthesis of other PBA NPs. For example, by using $K[Co(CN)_6]$ as cyanide ligands, $KCo^{2+}[Co^{3+}(CN)_6]$ and $KCu^{2+}[Co^{3+}(CN)_6]$ NPs with red and green colors could be synthesized with sizes of ∼30 and ∼46 nm (Figure 1b,e,f), and visible absorption peaks at about 516 and 765 nm (Figure 1c), respectively. Further, more PBA NPs such as $KNi^{2+}[Fe^{3+}(CN)_6]$, $KCo^{2+}[Fe^{3+}(CN)_6]$, $KFe_{0.12}{}^{2+}Cu_{0.88}{}^{2+}[Fe^{3+}(CN)_6]$, and $KFe_{0.11}{}^{2+}Co_{0.89}{}^{2+}[Fe^{3+}(CN)_6]$ with various colors could also be synthesized by using $K[Fe^{3+}(CN)_6]$ as cyanide ligands (Figures S3, S4, and S5).

The binding of capping agents on both PB and TiO_2 NPs benefits the high stability of the colloidal particles, which is essential for homogeneous mixing of the aqueous solution of NPs. However, a simple solution with mixed PB and TiO_2 NPs could not change color under extended UV irradiation, which is mainly due to nonclose contact between PB and TiO_2 particles in solution. We therefore cast the mixture on a solid substrate such as glass to form a solid film with significantly improved interparticle contact. Hydroxyethyl cellulose (HEC) and ethylene glycol (EG) were also introduced into the solid film, which could facilitate the film formation and improve the film smoothness. HEC also contributed additional benefit to slowdown the oxidation process by limiting the diffusion of ambient oxygen into the solid film.[17] The solid film showed considerable color change upon UV irradiation due to the improved contact, suggesting effective electron transfer between PB and TiO_2 (Figure 2a and Figure S6). The blue color disappeared rapidly upon UV irradiation under a typical laboratory 365 nm UV lamp (8 W, Spectroline EN-180), and the colorless film switched back by oxidation in ambient air. As shown in Figure 2b, the absorption peak of the solid film at ∼704 nm decreased in intensity with a longer irradiation time and eventually disappeared completely after 30 s of UV exposure as PB was reduced to PW. The absorption spectra of the colorless film gradually recovered in 12 h under ambient air (Figure 2c) due to the spontaneous oxidation of PW to PB by oxygen. The recoloration process could be further controlled according to the need in applications. For example, to accelerate the recoloration, the colorless solid film was heated in air at 120 °C, which could markedly enhance the recoloration rate, and the color could restore fully in 10 min (Figure S7). On the other hand, incorporating a larger amount of HEC into the film and/or covering the film with an additional HEC layer on the top surface can significantly slow down the recoloration process. For a sample prepared using the standard procedure described in the experimental section followed by an additional layer of ∼35 μm HEC (Figure S8), there was negligible oxidization of PW to PB at the first 3 days (Figure S9), and only 15.2% and 36.3% after 5 and 10 days, respectively. The ability of maintaining a considerably long colorless state affords great flexibility in practical applications. It should be noted that embedding the PBA/TiO_2 nanoparticles in HEC also brings additional benefit by minimizing their

DOI: 10.1021/acs.nanolett.6b03909
Nano Lett. 2017, 17, 755−761

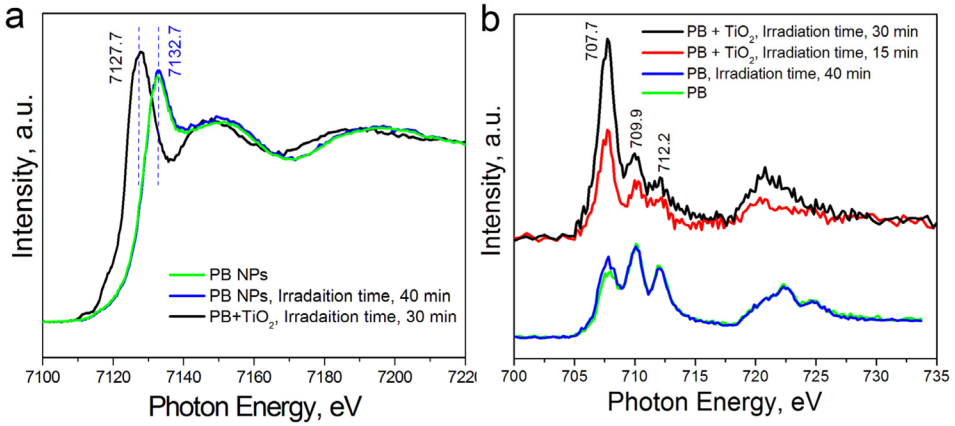

Figure 3. Color switching mechanism of the PB/TiO_2 NP mixture. (a) Fe *K*-edge and (b) Fe 2p *L*-edge XAS spectra of PB NPs and the PB/TiO_2 NP mixture.

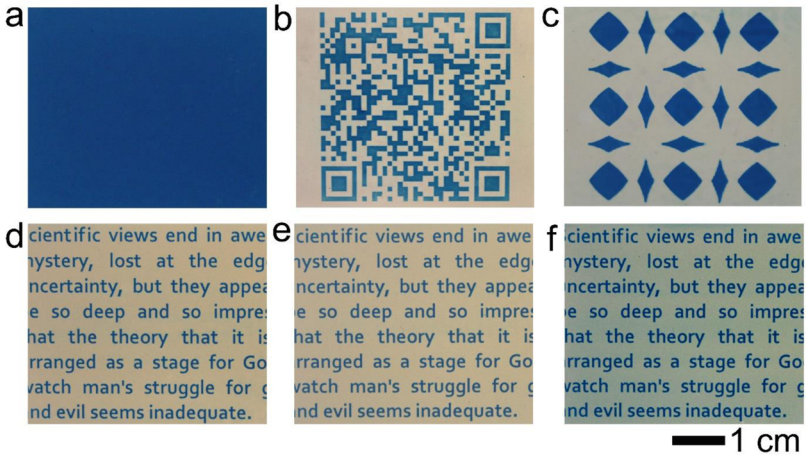

Figure 4. Printing and legibility of letters and patterns on the rewritable paper. (a) Digital photo of original rewritable paper. (b, c) Digital images of complex patterns printed on the rewritable paper. The image in b is a barcode linking to the authors' homepage. (d–f) Digital photos of a printed rewritable paper maintained in air for (d) 10 min, (e) 1 day, and (f) 2 days. The printed text is a quote by Richard Feynman.

potential toxicity. The decoloration and recoloration process were repeated in cycles to evaluate the reversibility and stability of the color switching system. Figure 2d plots the intensity of the main absorption peak under two different states, demonstrating unprecedented high reversibility and repeatability of the new color switching system. No obvious decrease except minor fluctuation in the absorption intensity was observed in the recovered state even after 80 consecutive switching cycles. We attribute the outstanding reversibility and repeatability of the current PCSS to the high photostability of PB and PBAs in comparison to the organic chromophores[40] and organic dyes[19] used in the previous systems.

X-ray absorption spectroscopy (XAS) was used as one of the most sensitive probes of electronic states to investigate the color switching mechanism of the PB/TiO_2 NP mixture. PB NPs and PB/TiO_2 NP mixtures were characterized by XAS at the Fe *K*-edge, as shown in Figure 3a. The spectrum displays the main features expected for Fe *K*-edge in PB: a very weak pre-edge peak (~7115 eV, 1s → 3d transitions) which is hardly detectable, then an intense whiteline feature (~7130 eV, 1s → 4p transitions), multiple-scattering structures after the whiteline feature, and finally the beginning of the EXAFS oscillations at higher energies.[41] No obvious change for Fe *K*-edge of PB NPs even under UV irradiation of 40 min demonstrates that PB is an ideal redox imaging media with high stability against photodegradation. After UV irradiation, a significant shift of the absorption edge of ~5 eV toward lower energies was observed for the TiO_2/PB NP mixture, clearly indicating reduction of PB to PW.[42,43] Fe *L*-edge XAS corresponds to the excitation of Fe 2p core electrons to the unoccupied 3d orbitals. The overall spectra line shape consists of features in two regions, L_3 around 710 eV and L_2 around 722 eV, resulting from the core-level spin–orbital coupling split (Figure 3b).[44] The Fe L_3-edge XAS spectrum of PB NPs presents overlapping features of Fe^{2+} and Fe^{3+} at 707.8, 710.1, and 712.2 eV, in which Fe^{2+} has a strong peak at ~707 eV while Fe^{3+} has a strong one at ~710 eV.[45,46] Fe *L*-edge of the PB NPs also shows no obvious change under UV irradiation, further demonstrating its stability. For the PB/TiO_2 NP mixture, the relative intensity of the peak at 707.7 eV increases with increasing UV irradiation time, while the relative intensity of the peaks at 709.7 and 712.2 decreases after UV irradiation, indicating the reduction of Fe^{3+} to Fe^{2+}.[44,45] The results of Fe L_3-edge XAS spectra clearly show the color switching mechanism, in which PB is reduced to PW under UV irradiation. The photoexcitation of TiO_2 NPs produces oxidative holes and reductive electrons, with the holes being captured by surface bound SEDs (P123 and its possible

DOI: 10.1021/acs.nanolett.6b03909
Nano Lett. 2017, 17, 755–761

derivatives) and the electrons being transferred to reduce PB to PW.

The current PCSS with unprecedented high reversibility and stability makes it ideal for constructing practical rewritable paper. To study the printing property, we first fabricated a prototype of rewritable paper by drop-casting an aqueous mixture of PB, TiO_2, HEC, and EG on a glass substrate with a size of 50 × 65 mm^2 (Figure 4a) according to a typical procedure described in the experimental section. As shown in Figures 4b–d, complex patterns and letters (font size: 11.5) in blue color can be printed successfully with very high resolution on the rewritable paper by UV irradiation through a photomask, which was pre-produced by ink-jet printing with a black ink on a transparent plastic film. In this case, the exposed regions turned to colorless PW while the unexposed regions retained the blue color of PB. For the particular sample in Figures 4d, the letters remained highly legible for at least 2 days under ambient conditions. The printed letters were still legible even after 4 days although the background gradually turned to light blue due to the slow oxidation of PW to PB by oxygen in ambient condition (Figure S10). Various complicated patterns can also be photoprinted on the rewritable paper with high resolution, as shown in Figure 4e–h. As mentioned previously, the legible time can be further improved by covering an additional HEC layer on the top surface of the rewritable paper to reduce the diffusions of ambient oxygen. The letters remained highly legible even for 5 days under ambient conditions, long enough for most temporary recording/reading purposes (Figure S11). Photoprinting of negative patterns or letters with high resolution can also be achieved by using an inverted photomask (Figure S12), demonstrating the future possibility of using focused beam of light for more flexible printing. Thanks to the colloidal nature of the PBAs and TiO_2 NPs, our PCSS could be conveniently cast to larger substrates (Figure S13), which is often required for practical applications. To demonstrate the high resolution of the photoprinting, we have printed microscale patterns through a chrome photomask using a commercial laboratory 365 nm UV lamp. Compared with the patterns on the original photomask (Figure S14), small features of ~5 μm could be perfectly photoprinted on the rewritable paper with sharp edges, as shown in Figure S15. Considering the high reversibility, repeatability, legibility, and resolution, the current new rewritable paper represents a big step forward toward practical applications.

Since PBAs share the same crystal structure and redox-driven color switching property as PB, we have synthesized a number of PBA NPs with various colors, including $KFe^{2+}_{0.12}Cu^{2+}_{0.88}[Fe^{3+}(CN)_6]$, $KFe^{2+}_{0.11}Co^{2+}_{0.89}[Fe^{3+}(CN)_6]$, $KNi^{2+}[Fe^{3+}(CN)_6]$, $KCo^{2+}[Fe^{3+}(CN)_6]$, $KCo^{2+}[Co^{3+}(CN)_6]$, and $KCu^{2+}[Co^{3+}(CN)_6]$, and explored their use as the imaging media. The solid films with various colors are shown in the insets of Figure S16. Interestingly, the $KFe^{2+}_{0.12}Cu^{2+}_{0.88}[Fe^{3+}(CN)_6]$, $KFe^{2+}_{0.11}Co^{2+}_{0.89}[Fe^{3+}(CN)_6]$, $KNi^{2+}[Fe^{3+}(CN)_6]$, and $KCo^{2+}[Fe^{3+}(CN)_6]$ NPs as imaging media show color switching between color and colorless state, while $KCo^{2+}[Co^{3+}(CN)_6]$ and $KCu^{2+}[Co^{3+}(CN)_6]$ NPs show one color to the other color. Letters with six colors can be photoprinted on the rewritable paper based on transition metal hexacyanoferrate NPs by UV irradiation through a photomask (Figure S16a–d) and hexacyanocobaltate NPs (Figure S16e,f) through an inverted photomask, respectively. Compared with previously demonstrated PCSS, we believe PBAs would provide various options of working colors for the rewritable paper.

Integrating PCSS directly into paper-based substrate is a big challenge because the color switching property is very sensitive to the microenvironments on a paper substrate.[24] This is particularly a significant issue of our previous color switching system based on organic dyes, which can only be applied to nonporous substrates such as glass and plastic sheets. When it is cast to the surface of conventional paper, the porous network of polyhydroxyl fibers absorbs dye molecules more preferentially than TiO_2 NPs, resulting in phase separation between TiO_2 NPs and the dye molecules and subsequently inefficient electron transfer and color switching (Figure S17a).[17] In the current system, the polyhydroxyl fibers adsorb both types of NPs without much preference. The optical microscopy image shows a homogeneous blue color on the paper, indicating the close contact between PB and TiO_2 NPs (Figure S17b). Compared with previous version of rewritable paper, the paper substrate for PB/TiO_2/HEC does not need additional pretreatment, further promoting the potential of the system for practical applications. An aqueous mixture of imaging media NPs, TiO_2 NPs, HEC, and EG is conveniently pasted on a paper substrate to fabricate a rewritable paper (50 × 65 mm^2). After drying and pressing, three kinds of practical rewritable paper were obtained with blue, green, and red colors by using PB, $KCu^{2+}[Co^{3+}(CN)_6]$, and $KCo^{2+}[Co^{3+}(CN)_6]$ NPs as the imaging media, respectively, as shown in Figure 5a,c,e. Letters with high resolution could be easily photoprinted on the rewritable paper (Figure 5), which maintained the flexibility of the conventional paper (Figure S18).

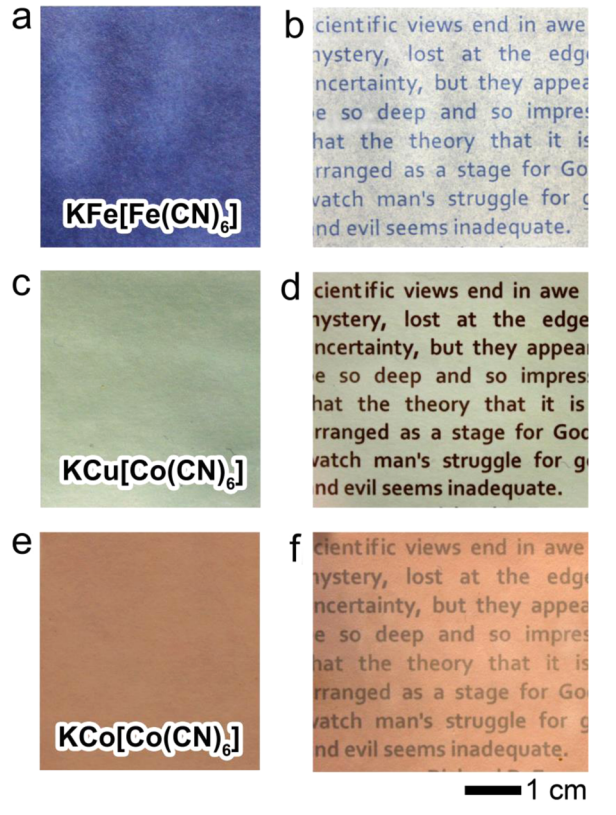

Figure 5. Rewritable paper fabricated using conventional paper as the substrate and different PBA NPs as the imaging media before and after light printing: (a, b) PB, (c, d) $KCu^{2+}[Co^{3+}(CN)_6]$, and (e, f) $KCo^{2+}[Co^{3+}(CN)_6]$ NPs. The printed text is a quote by Richard Feynman.

DOI: 10.1021/acs.nanolett.6b03909
Nano Lett. 2017, 17, 755–761

In summary, we have presented a new class of solid state PCSS by coupling the redox-driven color switching property of PB and PBA NPs with photocatalytic activity of TiO_2 NPs. The key to efficient electron transfer during color switching was found to be the assurance of close contact of PB/PBAs and the photocatalyst. We achieved such effective contact by synthesizing colloidal PB NPs using citric acid as the capping agent, mixing them with surface-engineered TiO_2 NPs, and then casting the mixture solution on substrates to form a solid film. In this way, the photogenerated electrons from TiO_2 NPs could be easily transferred to PB NPs and cause color change upon their reduction. The film can gradually return to its original color through oxidation by ambient oxygen. Since PB is very stable under UV irradiation, such color switching can be repeated over 80 times without apparent changes to the film properties such as color intensity and switching rate. With a similar crystal structure and redox-dependent color change property, PBA NPs can also be synthesized and used as imaging media to construct PCSS with many different working colors. In comparison to the previous color switching systems based on photoisomerization of chromophores or those depending on organic dyes, the current systems have key advantages in high reversibility and stability, easy handling, low cost, and toxicity. It also successfully addresses the phase separation issue with our previous system when applied to porous substrates so that the nanoparticle mixture can be conveniently cast onto the surfaces of a conventional paper to produce an ink-free light printable rewritable paper that has the same feel and appearance as the conventional paper, making it a significant step toward many practical applications. Letters/patterns can be effectively printed by UV irradiation through a mask, with a great potential to be printed directly by a scanning laser beam or an array of focused light beam from light-emitting diodes. The written content could remain legible for a considerably long time (over 5 days) as the recoloration through oxidation by ambient oxygen is rather slow, and if needed, the legible time can be further extended by covering the film with an additional polymer layer. Erasing the written content could be achieved quickly by heating the film at an elevated temperature (~120−150 °C, Figure S19). The rewritable paper can also be printed at high resolution: features of 5 μm could be achieved even using a commercial laboratory UV lamp. With all of these advantageous features, the current PCSS represents a new platform toward many practical applications involving temporary information recording and reading, such as newspapers, product life indicators, oxygen sensors, and various rewritable labels.

■ ASSOCIATED CONTENT

Supporting Information

The Supporting Information is available free of charge on the ACS Publications website at DOI: 10.1021/acs.nanolett.6b03909.

(PDF)

■ AUTHOR INFORMATION

Corresponding Authors

*E-mail address: wangws@sdu.edu.cn.

*E-mail address: yadong.yin@ucr.edu. Fax: +1-951-827-4713.

ORCID

Jinghua Guo: 0000-0002-8576-2172

Yadong Yin: 0000-0003-0218-3042

Notes

The authors declare no competing financial interest.

■ ACKNOWLEDGMENTS

Y.Y. is grateful for the support from the U.S. Department of Energy, Office of Science, Basic Energy Sciences, Chemical Sciences, Geosciences, & Biosciences (CSGB) Division, under Award No. DE-SC0002247. Acknowledgment is also made to the Donors of the American Chemical Society Petroleum Research Fund for partial support of this research. W.W. is thankful for the financial support from the National Natural Science Foundation of China (No. 21671120). The work performed on BL8.0.1.3, 6.3.1.2, and 10.3.2 at the Advanced Light Source is supported by the Director, Office of Science, Office of Basic Energy Sciences, of the U.S. Department of Energy under Contract No. DE-AC02-05CH11231. We thank Matthew Marcus, Sirine Fakra, and Josep Roque-Rosell for the technical support at the ALS beamlines.

■ REFERENCES

(1) Yao, J. N.; Hashimoto, K.; Fujishima, A. *Nature* **1992**, *355* (6361), 624−626.

(2) Bu, J. X.; Watanabe, K.; Hayasaka, H.; Akagi, K. *Nat. Commun.* **2014**, *5*, 2799.

(3) Dong, H.; Zhu, H.; Meng, Q.; Gong, X.; Hu, W. *Chem. Soc. Rev.* **2012**, *41*, 1754−1808.

(4) Jia, C. C.; Migliore, A.; Xin, N.; Huang, S. Y.; Wang, J. Y.; Yang, Q.; Wang, S. P.; Chen, H. L.; Wang, D. M.; Feng, B. Y.; Liu, Z. R.; Zhang, G. Y.; Qu, D. H.; Tian, H.; Ratner, M. A.; Xu, H. Q.; Nitzan, A.; Guo, X. F. *Science* **2016**, *352* (6292), 1443−1445.

(5) Baroncini, M.; d'Agostino, S.; Bergamini, G.; Ceroni, P.; Comotti, A.; Sozzani, P.; Bassanetti, I.; Grepioni, F.; Hernandez, T. M.; Silvi, S.; Venturi, M.; Credi, A. *Nat. Chem.* **2015**, *7* (8), 634−640.

(6) Kundu, P. K.; Samanta, D.; Leizrowice, R.; Margulis, B.; Zhao, H.; Borner, M.; Udayabhaskararao, T.; Manna, D.; Klajn, R. *Nat. Chem.* **2015**, *7* (8), 646−652.

(7) Sun, H. B.; Liu, S. J.; Lin, W. P.; Zhang, K. Y.; Lv, W.; Huang, X.; Huo, F. W.; Yang, H. R.; Jenkins, G.; Zhao, Q.; Huang, W. *Nat. Commun.* **2014**, *5*, 3601.

(8) Ohko, Y.; Tatsuma, T.; Fujii, T.; Naoi, K.; Niwa, C.; Kubota, Y.; Fujishima, A. *Nat. Mater.* **2003**, *2* (1), 29−31.

(9) Chen, S. J.; Chen, L. J.; Yang, H. B.; Tian, H.; Zhu, W. H. *J. Am. Chem. Soc.* **2012**, *134* (33), 13596−13599.

(10) DeForest, C. A.; Tirrell, D. A. *Nat. Mater.* **2015**, *14* (5), 523−531.

(11) Diaz, S. A.; Gillanders, F.; Jares-Erijman, E. A.; Jovin, T. M. *Nat. Commun.* **2015**, *6*, 6036.

(12) Garcia-Fernandez, L.; Herbivo, C.; Arranz, V. S.; Warther, D.; Donato, L.; Specht, A.; del Campo, A. *Adv. Mater.* **2014**, *26* (29), 5012−5017.

(13) Rao, Y. L.; Horl, C.; Braunschweig, H.; Wang, S. N. *Angew. Chem., Int. Ed.* **2014**, *53* (34), 9086−9089.

(14) Kobatake, S.; Takami, S.; Muto, H.; Ishikawa, T.; Irie, M. *Nature* **2007**, *446* (7137), 778−781.

(15) Li, K.; Xiang, Y.; Wang, X. Y.; Li, J.; Hu, R. R.; Tong, A. J.; Tang, B. Z. *J. Am. Chem. Soc.* **2014**, *136* (4), 1643−1649.

(16) Meng, F.; Hervault, Y.-M.; Shao, Q.; Hu, B.; Norel, L.; Rigaut, S.; Chen, X. *Nat. Commun.* **2014**, *5*, 3023.

(17) Wang, W.; Xie, N.; He, L.; Yin, Y. *Nat. Commun.* **2014**, *5*, 5459.

(18) Wang, W.; Ye, Y.; Feng, J.; Chi, M.; Guo, J.; Yin, Y. *Angew. Chem., Int. Ed.* **2015**, *54* (4), 1321−1326.

(19) Wang, W.; Ye, M.; He, L.; Yin, Y. *Nano Lett.* **2014**, *14*, 1681−1686.

(20) White paper: Environmental issues associated with toner and ink Usage (Preton Ltd., 2010).

(21) RISI. World pulp Annual historical date (RISI, 2010).

DOI: 10.1021/acs.nanolett.6b03909
Nano Lett. 2017, 17, 755−761

(22) Garcia-Amorós, J.; Swaminathan, S.; Raymo, F. M. *Dyes Pigm.* **2014**, *106*, 71−73.
(23) Kishimura, A.; Yamashita, T.; Yamaguchi, K.; Aida, T. *Nat. Mater.* **2005**, *4* (7), 546−549.
(24) Sheng, L.; Li, M. J.; Zhu, S. Y.; Li, H.; Xi, G.; Li, Y. G.; Wang, Y.; Li, Q. S.; Liang, S. J.; Zhong, K.; Zhang, S. X. A. *Nat. Commun.* **2014**, *5*, 3044.
(25) Sarantis, H. Business guide to paper reduction, ForestEthics, 2002.
(26) Kawashima, I.; Takahashi, H.; Hirano, S.; Matsushima, R. *J. Soc. Inf. Disp.* **2004**, *12* (1), 81−85.
(27) Kinashi, K.; Horiguchi, T.; Tsutsui, K.; Ishida, K.; Ueda, Y. *J. Photochem. Photobiol., A* **2010**, *213* (2−3), 189−193.
(28) Kohno, Y.; Tamura, Y.; Matsushima, R. *J. Photochem. Photobiol., A* **2009**, *201*, 98−101.
(29) Shokouhimehr, M.; Soehnlen, E. S.; Hao, J.; Griswold, M.; Flask, C.; Fan, X.; Basilion, J. P.; Basu, S.; Huang, S. D. *J. Mater. Chem.* **2010**, *20* (25), 5251−5259.
(30) Bai, L.; Jin, L.; Han, L.; Dong, S. *Energy Environ. Sci.* **2013**, *6* (10), 3015−3021.
(31) Lee, H.-W.; Wang, R. Y.; Pasta, M.; Lee, S. W.; Liu, N.; Cui, Y. *Nat. Commun.* **2014**, *5*, 5280.
(32) Wang, J.; Zhang, L.; Yu, L.; Jiao, Z.; Xie, H.; Lou, X. W.; Sun, X. W. *Nat. Commun.* **2014**, *5*, 4921.
(33) Han, L.; Guo, S.; Wang, P.; Dong, S. *Adv. Energy Mater.* **2015**, *5* (2), 1400424.
(34) Kim, L. T. T.; Gabrielli, C.; Perrot, H.; Garcia-Jareno, J.; Vicente, F. *Electrochim. Acta* **2012**, *84*, 35−48.
(35) Stilwell, D. E.; Park, K. H.; Miles, M. H. *J. Appl. Electrochem.* **1992**, *22* (4), 325−331.
(36) Itaya, K.; Shibayama, K.; Akahoshi, H.; Toshima, S. *J. Appl. Phys.* **1982**, *53*, 804−805.
(37) Itaya, K.; Uchida, I.; Toshima, S.; Rue, R. *J. Electrochem. Soc.* **1984**, *131*, 2086−2091.
(38) Fujishima, A.; Rao, T.; Tryk, D. *J. Photochem. Photobiol., C* **2000**, *1* (1), 1−21.
(39) Wessells, C. D.; Huggins, R. A.; Cui, Y. *Nat. Commun.* **2011**, *2*, 550.
(40) Zhang, J. J.; Zou, Q.; Tian, H. *Adv. Mater.* **2013**, *25* (3), 378−399.
(41) Cafun, J. D.; Lejeune, J.; Itie, J. P.; Baudelet, F.; Bleuzen, A. *J. Phys. Chem. C* **2013**, *117* (38), 19645−19655.
(42) Gervais, C.; Languille, M. A.; Moretti, G.; Reguer, S. *Langmuir* **2015**, *31* (29), 8168−8175.
(43) Hayakawa, K.; Hatada, K.; D'Angelo, P.; Della Longa, S.; Natoli, C. R.; Benfatto, M. *J. Am. Chem. Soc.* **2004**, *126* (47), 15618−15623.
(44) Liu, X. S.; Wang, D. D.; Liu, G.; Srinivasan, V.; Liu, Z.; Hussain, Z.; Yang, W. L. *Nat. Commun.* **2013**, *4*, 2568.
(45) Wang, L.; Song, J.; Qiao, R.; Wray, L. A.; Hossain, M. A.; Chuang, Y.-D.; Yang, W.; Lu, Y.; Evans, D.; Lee, J.-J.; Vail, S.; Zhao, X.; Nishijima, M.; Kakimoto, S.; Goodenough, J. B. *J. Am. Chem. Soc.* **2015**, *137* (7), 2548−2554.
(46) Crocombette, J. P.; Pollak, M.; Jollet, F.; Thromat, N.; Gautiersoyer, M. *Phys. Rev. B: Condens. Matter Mater. Phys.* **1995**, *52* (5), 3143−3150.

DOI: 10.1021/acs.nanolett.6b03909
Nano Lett. 2017, 17, 755−761